ABCM Symposium Series in Mechatronics - Vol. 1 - pp.321-330
Copyright © 2004 by ABCM

MODAL VIBRATION CONTROL IN PERIODIC TIME-VARYING STRUCTURES WITH FOCUS ON ROTOR-BLADE SYSTEMS

René Hardam Christensen
MEK - Department of Mechanical Engineering, DTU - Technical University Denmark, DK-2800 Kgs. Lyngby, Denmark
rhc@mek.dtu.dk

Ilmar Ferreira Santos
MEK - Department of Mechanical Engineering, DTU - Technical University Denmark, DK-2800 Kgs. Lyngby, Denmark
ifs@mek.dtu.dk

Abstract. *In this paper an active controller for a periodic time-variant coupled rotor-blade system is designed. A periodic modal state feedback control scheme is designed based on a modal transformation of the system into a linear time-invariant formulation. The transformation makes it possible to design the controller using classical linear control techniques. Moreover, it provides the possibility to reduce the order of the system resulting in a simpler and more implementable controller. Non-measurable state variables are estimated using a periodic time-varying state observer designed by a similar procedure. The applicability of the controller design methodology is evaluated by numerical simulations on a coupled periodic time-variant rotor-blade system. A simulation model for such a system is formulated and three different control schemes are designed using the described methodology. The results obtained demonstrate that the designed controllers are capable to cope with the time periodicity of the system. Furthermore, the results show that specific vibration modes can be selected and controlled separately and very effectively.*

Keywords. *Modal vibration control, Periodic time-variant, Rotor-blade systems.*

1. Introduction

Active modal control of vibrations in flexible structures has been extensively studied for several decades and applied to various types of systems (Balas, 1978; Firoozian and Stanway, 1988; Kaneko and Kano, 1989; Chantalakhana and Stanway, 2000; Khulief, 2001) suppressing vibrations among others in flexible rotors, plates and rotating beams. Most of the work reported deals only with linear time-invariant systems, however, many mechanical systems are non-linear and time-variant. One example of such is coupled rotor-blade systems, where the flexible motion of the blades is coupled to rigid body motion of the rotor shaft. Rotating at constant speed such systems are often linear and periodic time-variant, the inertia and the stiffness coefficients used to represent the rotor-blade dynamics are time-depending and change periodically. Therefore, in order to reduce vibrations by means of active control a time-variant control strategy, capable to cope with this time-periodicity and with the fact that the natural frequencies of the blades strongly change with the rotational speed, due to the stiffening effect, has to be adopted.

The most comprehensive way of dealing with active control of such systems would be by applying adaptive learning control techniques for general non-linear time-variant systems. However, several control methodologies, directly pointed towards periodic systems, have been reported during the last two decades. For instance, an optimal periodic controller is designed in (Arcara et al., 2000) by solving a periodic Ricatti equation and a periodic $\mathcal{H}_\infty$-controller is designed in (Bittanti and Cuzzola, 2002). Other researchers make use of a transformation of the periodic system into a time-invariant form. Hereby, linear time-invariant control technique is applied for the controller design. Calico and Wiesel (1984) describes a technique for designing a pole placement state feedback controller by gain selection based on a modal transformation of the periodic system. In order to avoid real time estimation of the periodic state variables, Calise et al. (1992) proposed a design technique for an optimal output feedback controller with fixed gains based on a modal transformation of the periodic system. Sinha and Joseph (1994) reported a method for designing periodic state feedback controllers using a more general and less cumbersome Lyapunov-Floquet transformation method based on Chebyshev polynomials. The efficiency of this methodology has been investigated in different types of systems i.e. to control a parametrically excited beam (Marghitu et al., 1999) and to control vibrations in a bladed disk assembly (Szász and Flowers, 2001).

In this paper, a periodic time-variant modal controller is designed, aiming at attenuating vibrations in a coupled rotor-blade system. Moreover, while designing modal controllers, it is not always desired to address and suppress all vibration modes, but only those which can cause significant damages to the machines. In this framework, the aim of this work is to design a modal controller capable to address and suppress specific selected vibration modes in the periodic system. Such a selection minimizes the order, complexity and energy consumption of the controller. Therefore, by combining elements from the previously reported works, a state feedback controller is designed similar to the method presented by Sinha and Joseph (1994), based on Chebyshev polynomials. However, in order to address the modal control concept, the system is transformed into a time-invariant form by the modal transformation technique for periodic systems, as presented by Calise et al. (1992) and described in details by Xu and Gasch (1995). The efficiency of applying this modal transformation for analysing and mathematically explaining parametric vibrations in coupled rotor-blade systems is described by Saracho and Santos (2003). Among the advantages of using this modal transformation for the controller design procedure one can mention that it allows a straightforward method for analysing the modal controllability and observability of the time-

varying system and provides a better physical interpretation and visualisation of the time-varying mode shapes which are very useful e.g. for decisions regarding actuator and sensor placement. Therefore, when designing active controllers for this special kind of mechanical system the periodic modal transformation becomes a very powerful tool.

2. Mathematical Model

A mechanical model of the considered coupled rotor-blade system is shown in Fig. (1a). The rotor-shaft is assumed to be rigid and is mounted in a hub performing planar movement in the xy-plane. Four identical flexible blades with tip masses are radially attached to the rigid rotor and the motion of the blades are also assumed to be planar. The vibrations of the structure are controlled by up to six forces acting onto the hub (F_{h_x} and F_{h_y}) and onto each of the blades (F_{b_1}, F_{b_2}, F_{b_3} and F_{b_4}). Whether all these six forces (actuators) have to be applied to the system in order to control the vibrations, or whether it is sufficient to apply only some of them, is analysed in section 5.

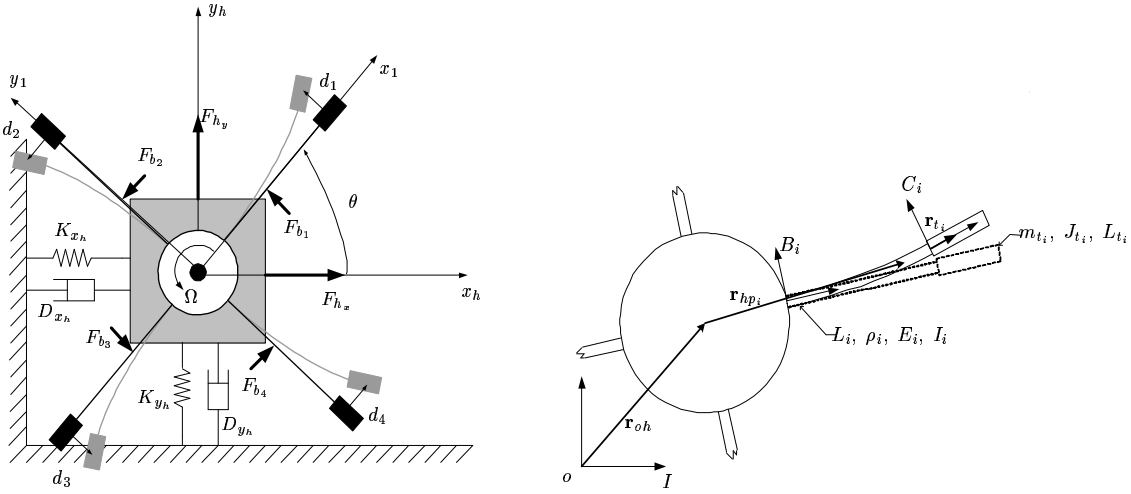

(a) (b)

Figure 1: (a) Mechanical model of the coupled rotor-blade system - x_h, y_h, d_1, d_2, d_3, d_4 are the minimal coordinates for describing the rotor-blade system dynamics; F_{h_x}, F_{h_y}, F_{b_1}, F_{b_2}, F_{b_3}, F_{b_4} are the active control forces and D_{x_h}, D_{y_h}, K_{x_h}, K_{y_h} are the damping and stiffness of the hub foundation. (b) The inertial and moving reference systems and position vectors used for derivation of the dynamic model. The parameters L_i, ρ_i, E_i, I_i and L_{t_i}, m_{t_i}, J_{t_i} relate to blades and tip masses.

The equations of motion for the rotor-blade system are derived using Lagrangian dynamics. Figure (1b) shows the coordinate systems and position vectors used to develop the model. Index I denotes the inertial reference frame attached to the hub and B_i and C_i denotes auxiliary coordinate systems attached to the rotor and to the tip masses.

The kinetic energy of the assembly is given by a sum of three contributions: (I) the rotor kinetic energy T_r; (II) the blades kinetic energy T_b and (III) the tip masses kinetic energy T_t. Axial elongation of the blades as well as the blade inertia are neglected in T_b. The total kinetic energy then is $T = T_r + T_b + T_t$, where:

$$T_r = \tfrac{1}{2} J_h \dot{\theta}^2 + \tfrac{1}{2} m_h \ {}_I\dot{\mathbf{r}}_{oh} \cdot {}_I\dot{\mathbf{r}}_{oh} \tag{1}$$

$$T_b = \sum_{i=1}^{4} \tfrac{1}{2} \rho_i \int_0^{L_i} {}_I\dot{\mathbf{r}}_{op_i}(x_i) \cdot {}_I\dot{\mathbf{r}}_{op_i}(x_i)\, dx_i \tag{2}$$

$$T_t = \sum_{i=1}^{4} \left[\tfrac{1}{2} m_{t_i} \ {}_I\dot{\mathbf{r}}_{ot_i} \cdot {}_I\dot{\mathbf{r}}_{ot_i} + \tfrac{1}{2} J_{t_i} \left(\dot{\theta} + \tfrac{\partial}{\partial x_i} (\dot{y}_i(L_i)) \right)^2 \right] \tag{3}$$

The potential energy of the assembly consists also of three contributions: (I) the potential strain energy due to the elastic deformation of the blades V_e; (II) the gravity potential energy V_{gr} and (III) the geometric deformation potential energy V_g. The last term is required to take into account the centrifugal stiffening of the blades, which results in an increase of the blade natural frequencies as a function of the rotational speed (Saracho and Santos, 2001). Denoting the gravity vector ${}_I\mathbf{g}$ and the normal force acting on the beams by $N(x_i)$ the total potential energy is $V = V_e + V_{gr} + V_g$, where:

$$V_e = \sum_{i=1}^{4} \int_0^{L_i} \tfrac{1}{2} E_i I_i \left(\tfrac{\partial^2 y_i}{\partial x_i^2} \right)^2 dx_i \tag{4}$$

$$V_{gr} = m_{h_y} \ {}_I\mathbf{g} \cdot {}_I\mathbf{r}_{oh} + \sum_{i=1}^{4} \left[m_{t_i} \ {}_I\mathbf{g} \ \cdot {}_I\mathbf{r}_{ot_i} + \rho \int_0^{L_i} {}_I\mathbf{g} \cdot {}_I\mathbf{r}_{op_i}(x_i) dx_i \right] \tag{5}$$

$$V_g = \sum_{i=1}^{4} \tfrac{1}{2} \int_0^{L_i} N(x_i) \left(\tfrac{\partial y_i}{\partial x_i} \right)^2 dx_i \tag{6}$$

The dynamic model is discretized by expressing the blade-bending deformation in terms of the n lowest mode shapes, that is:

$$d_i(t,x_i) = \sum_{j=1}^{n} q_{ji}(t)\varphi_j(x_i) \quad \text{for} \quad i = 1,2,3,4 \quad \text{and} \quad 0 \le x_i \le L_i \tag{7}$$

where n is the number of modes, $q_{ji}(t)$ and $\varphi_j(x_i)$ are the modal coordinate and the mode shape function for the j-th mode of the i-th blade deflection, respectively. The general equations of motion for the coupled rotor-blade system are non-linear, time-varying and functions of the rotor position θ, the rotational speed Ω and acceleration $\dot{\Omega}$. Therefore, the equations of motion are written as:

$$\mathbf{M}(t)\ddot{\mathbf{z}}(t) + \mathbf{H}(t,\Omega)\dot{\mathbf{z}}(t) + \mathbf{K}(t,\Omega,\dot{\Omega})\mathbf{z}(t) = \mathbf{P}(t,\Omega,\dot{\Omega}) + \mathbf{Q}\mathbf{u}(t) \tag{8}$$

where $\mathbf{z}(t)_{(N\times 1)} = \{x_h,\, y_h,\, \mathbf{q}_1,\, \mathbf{q}_2,\, \mathbf{q}_3,\, \mathbf{q}_4\}^T$ is a vector of generalized coordinates and the vector of control forces acting on the assembly is $\mathbf{u}(t)_{(6\times 1)} = \{F_{h_x},\, F_{h_y},\, F_{b_1},\, F_{b_2},\, F_{b_3},\, F_{b_4}\}^T$. Detailed information about the modal matrices is given in the appendix. Rewriting the system Eq. (8) into a state-space form, yields:

$$\dot{\mathbf{x}}(t) = \mathbf{A}(t)\mathbf{x}(t) + \mathbf{B}(t)\mathbf{u}(t) + \mathbf{F}(t) \tag{9}$$

with the vector of state variables $\mathbf{x}(t)^T_{(2N\times 1)} = \{\mathbf{z}(t)^T\ \dot{\mathbf{z}}(t)^T\}$ and the system matrices:

$$\mathbf{A}(t)_{(2N\times 2N)} = \begin{bmatrix} \mathbf{0} & \mathbf{I} \\ -\mathbf{M}(t)^{-1}\mathbf{K}(t) & -\mathbf{M}(t)^{-1}\mathbf{H}(t) \end{bmatrix};\ \mathbf{B}(t)_{(2N\times 6)} = \begin{bmatrix} \mathbf{0} \\ \mathbf{M}(t)^{-1}\mathbf{Q} \end{bmatrix};\ \mathbf{F}(t)_{(2N\times 1)} = \begin{Bmatrix} \mathbf{0} \\ \mathbf{M}(t)^{-1}\mathbf{P}(t) \end{Bmatrix} \tag{10}$$

The output equation for the system is given by $\mathbf{y}(t) = \mathbf{C}\mathbf{x}(t)$, where $\mathbf{C}$ is defined in such a way that the outputs are given by the position of the hub and the tip point deflections of the blades $\mathbf{y}(t)_{(6\times 1)} = \{x_h,\, y_h,\, d_1,\, d_2,\, d_3,\, d_4\}^T$.

3. Reduced Modal Model for Control

The model Eq. (9) is transformed into a system of independent equations of motion, where each equation represents one vibration mode by using a periodic modal transformation. This modal formulation is obtained by introducing a new vector of modal state variables $\boldsymbol{\xi}(t)$ defined by $\mathbf{x}(t) = \mathbf{R}(t)\boldsymbol{\xi}(t)$ where $\mathbf{R}(t)$ is the right modal matrix. Introducing this new state vector, the system is rewritten to the form:

$$\dot{\boldsymbol{\xi}}(t) = \boldsymbol{\mathcal{A}}\boldsymbol{\xi}(t) + \boldsymbol{\mathcal{B}}(t)\mathbf{u}(t) + \boldsymbol{\mathcal{F}}(t)\ \ ;\ \ \mathbf{y}(t) = \boldsymbol{\mathcal{C}}(t)\boldsymbol{\xi}(t) \tag{11}$$

where $\boldsymbol{\mathcal{A}} = [\mathbf{L}^T(t)\mathbf{A}(t)\mathbf{R}(t) - \mathbf{L}^T(t)\dot{\mathbf{R}}(t)]$ is a diagonal matrix containing the eigenvalues of $\mathbf{A}(t)$ along the diagonal, $\boldsymbol{\mathcal{B}}(t) = \mathbf{L}^T(t)\mathbf{B}(t)$ is the modal control input matrix, $\boldsymbol{\mathcal{F}}(t) = \mathbf{L}^T(t)\mathbf{F}(t)$ is the vector of modal forces and $\boldsymbol{\mathcal{C}}(t) = \mathbf{C}\mathbf{R}(t)$ is the modal output matrix. Due to the time-periodicity of the system the right $\mathbf{R}(t)$ and left modal matrix $\mathbf{L}^T(t)$ are time-periodic. These can be determined using Hill's method of infinite determinants (Saracho and Santos, 2003; Xu and Gasch, 1995). Hereby the modal matrices are written as:

$$\mathbf{R}(t) = \mathbf{R}(t+T) = \sum_{j=-n}^{n} \mathbf{R}_j \mathrm{e}^{ij\Omega t} \quad \text{and} \quad \mathbf{R}(t)\mathbf{L}^T(t) = \mathbf{I} \tag{12}$$

In order to reduce the order of the controller and state observer the system, Eq. (14), is reorganized into a subset of controlled modes and a set of residual modes, denoted by the indices c and r, respectively. The controller is then designed to suppress only the selected vibration modes, thus considering remaining insignificant, non-controllable or non-observable modes as residual modes. Naturally such an order reduction implies that precautions have to be taken in order to avoid control and observation spill-over problems. Therefore, it might be necessary to implement for instance band-pass filters to eliminate excitation of non-controlled modes or to eliminate residual modes in the measured variables. The reduced modal system is written as:

$$\begin{Bmatrix} \dot{\boldsymbol{\xi}}_c(t) \\ \dot{\boldsymbol{\xi}}_r(t) \end{Bmatrix} = \begin{bmatrix} \boldsymbol{\mathcal{A}}_c & \mathbf{0} \\ \mathbf{0} & \boldsymbol{\mathcal{A}}_r \end{bmatrix} \begin{Bmatrix} \boldsymbol{\xi}_c(t) \\ \boldsymbol{\xi}_r(t) \end{Bmatrix} + \begin{bmatrix} \boldsymbol{\mathcal{B}}_c(t) \\ \boldsymbol{\mathcal{B}}_r(t) \end{bmatrix} \mathbf{u}(t) + \begin{Bmatrix} \boldsymbol{\mathcal{F}}_c(t) \\ \boldsymbol{\mathcal{F}}_r(t) \end{Bmatrix} \tag{13}$$

Due to the complex eigenvalues and eigenvectors of the system resulting in complex coefficients, the reduced model of controlled modes is rewritten into a real form by separating real and imaginary parts. This real model is expressed by:

$$\dot{\bar{\boldsymbol{\xi}}}(t) = \bar{\boldsymbol{\mathcal{A}}}\bar{\boldsymbol{\xi}}(t) + \bar{\boldsymbol{\mathcal{B}}}(t)\mathbf{u}(t) + \bar{\boldsymbol{\mathcal{F}}}(t) \quad ; \quad \bar{\mathbf{y}}(t) = \bar{\boldsymbol{\mathcal{C}}}(t)\bar{\boldsymbol{\xi}}(t) \tag{14}$$

where the state vector and the matrices $\bar{\boldsymbol{\mathcal{A}}}$, $\bar{\boldsymbol{\mathcal{B}}}(t)$ and $\bar{\boldsymbol{\mathcal{C}}}(t)$ are given by:

$$\bar{\boldsymbol{\xi}}(t)_{(2N_c\times 1)} = \left[\, \Re(\boldsymbol{\xi}_{c,1}),\ \Im(\boldsymbol{\xi}_{c,1}),\ \Re(\boldsymbol{\xi}_{c,2}),\ \Im(\boldsymbol{\xi}_{c,2}),\ \ldots,\ \Re(\boldsymbol{\xi}_{c,N_c}),\ \Im(\boldsymbol{\xi}_{c,N_c}) \,\right]^T \tag{15}$$

$$\bar{\boldsymbol{\mathcal{A}}}_{(2N_c\times 2N_c)} = \begin{bmatrix} \ddots & & \mathbf{0} \\ & \bar{\boldsymbol{\mathcal{A}}}_{ii} & \\ \mathbf{0} & & \ddots \end{bmatrix} \quad \text{where} \quad \bar{\boldsymbol{\mathcal{A}}}_{ii} = \begin{bmatrix} \Re(\lambda_i) & -\Im(\lambda_i) \\ \Im(\lambda_i) & \Re(\lambda_i) \end{bmatrix} \tag{16}$$

$$\bar{\boldsymbol{\mathcal{B}}}(t)_{(2N_c\times 6)} = \left[\ \Re(\boldsymbol{\mathcal{B}}_{c,1}),\ \ \Im(\boldsymbol{\mathcal{B}}_{c,1})\ \ \ldots\ \ \Re(\boldsymbol{\mathcal{B}}_{c,N_c}),\ \ \Im(\boldsymbol{\mathcal{B}}_{c,N_c})\ \right]^T \tag{17}$$

$$\bar{\boldsymbol{\mathcal{C}}}(t)_{(6\times 2N_c)} = \left[\ \Re(\boldsymbol{\mathcal{C}}_{c,1}),\ \ -\Im(\boldsymbol{\mathcal{C}}_{c,1})\ \ \ldots\ \ \Re(\boldsymbol{\mathcal{C}}_{c,N_c}),\ \ -\Im(\boldsymbol{\mathcal{C}}_{c,N_c})\ \right] \tag{18}$$

N_c denotes the number of controlled modes.

4. Active Controller Design

4.1. Modal Controllability and Observability

In order to determine the minimum number and optimal placement of actuators and sensors the modal controllability and observability may be analysed. General speaking, the system is modal controllable if no row of the modal control matrix consists only of zeros and all modes are observable if no column of the modal output matrix consists only of zeros. However, these are poor measures of the modal controllability and observability. Better indices are provided by (Hamdan and Nayfeh, 1989) who state quantitative indices of how controllable and observable a specific mode is, from all inputs and outputs, respectively. Such measures are given by:

$$\mathrm{MC}_i(t) = \mathrm{norm}\left(\frac{\mathbf{l}_i^T(t)\cdot\mathbf{B}(t)}{\parallel \mathbf{l}_i^T(t)\parallel}\right) \quad ; \quad \mathrm{MO}_i(t) = \mathrm{norm}\left(\frac{\mathbf{C}\cdot\mathbf{r}_i(t)}{\parallel \mathbf{r}_i(t)\parallel}\right) \tag{19}$$

where $\mathbf{r}_i(t)$ and $\mathbf{l}_i^T(t)$ are the i'th right and left eigenvector, respectively.

In general, the controllability and observability indices $\mathrm{MC}_i(t)$ and $\mathrm{MO}_i(t)$ are time-variant. However, for the actual coupled rotor-blade system the indices become constant due to the periodicity of the model matrix $\mathbf{B}(t)$ and the modal matrices $\mathbf{R}(t)$ and $\mathbf{L}^T(t)$ with the same length of period $1/\Omega$.

4.2. Time-Periodic Modal State Controller

Using the periodic oscillatory modal model, Eq. (14), a time-periodic controller for the original periodic system, Eq. (9), is designed using traditional time-invariant control technique. A time-periodic state feedback controller is designed by a methodology similar to the method used in (Sinha and Joseph, 1994), however, based on the modal transformed model. The time-variant state feedback control law is defined by:

$$\mathbf{u}(t) = \bar{\boldsymbol{\mathcal{G}}}(t)\bar{\boldsymbol{\xi}}(t) \tag{20}$$

Substituting $\bar{\boldsymbol{\mathcal{B}}}(t)$ by a constant matrix $\bar{\boldsymbol{\mathcal{B}}}_0$, i.e. given by the value of $\bar{\boldsymbol{\mathcal{B}}}(t)$ at a specific instant of time, and neglecting the modal force vector the modal model, Eq. (14), is given by:

$$\dot{\bar{\boldsymbol{\xi}}}(t) = \bar{\boldsymbol{\mathcal{A}}}\bar{\boldsymbol{\xi}}(t) + \bar{\boldsymbol{\mathcal{B}}}_0\mathbf{u}_0(t) \tag{21}$$

If the system is non-controllable or only weakly controllable at specific instants of time the matrix $\bar{\boldsymbol{\mathcal{B}}}_0$ has to be carefully chosen in order to avoid troubles. For this time-invariant system, Eq. (21), a control law is defined by:

$$\mathbf{u}_0(t) = \bar{\boldsymbol{\mathcal{G}}}_0\bar{\boldsymbol{\xi}}(t) \tag{22}$$

where $\bar{\boldsymbol{\mathcal{G}}}_0$ is a constant gain controller designed by traditional linear time-invariant control technique, for instance by LQ-design.

By 'equalizing' the periodic oscillatory system, Eq. (14), and the rewritten time-invariant system, Eq. (21), the constant gain controller is transformed into a periodic form. The periodic controller gain matrix then is:

$$\bar{\boldsymbol{\mathcal{G}}}(t) = [\bar{\boldsymbol{\mathcal{B}}}^T(t)\bar{\boldsymbol{\mathcal{B}}}(t)]^{-1}\bar{\boldsymbol{\mathcal{B}}}^T(t)\bar{\boldsymbol{\mathcal{B}}}_0\bar{\boldsymbol{\mathcal{G}}}_0 \tag{23}$$

4.3. Time-Periodic Modal State Observer

All state variables are not directly measureable. Therefore a deterministic time-periodic observer is designed to estimate the state variables. The periodic observer equation is given by:

$$\dot{\hat{\bar{\boldsymbol{\xi}}}}(t) = \bar{\boldsymbol{\mathcal{A}}}\hat{\bar{\boldsymbol{\xi}}}(t) + \bar{\boldsymbol{\mathcal{B}}}(t)\mathbf{u}(t) + \bar{\boldsymbol{\mathcal{F}}}(t) + \bar{\boldsymbol{\mathcal{G}}}_{obs}(t)\left(\mathbf{y}(t) - \bar{\boldsymbol{\mathcal{C}}}(t)\hat{\bar{\boldsymbol{\xi}}}(t)\right) \tag{24}$$

where $\hat{\bar{\boldsymbol{\xi}}}(t)$ denotes the estimated state variables, $\mathbf{y}(t)$ the measured variables and $\bar{\boldsymbol{\mathcal{G}}}_{obs}(t)$ the observer gain matrix.

It is well known that the observer gain matrix for a time-invariant system can be determined by designing a controller

for the dual system. Using this property the periodic time-varying observer gain matrix can be designed by a procedure similar to the controller design procedure. The dual system is given by:

$$\dot{\bar{\boldsymbol{\xi}}}_d(t) = \bar{\boldsymbol{\mathcal{A}}}^T \bar{\boldsymbol{\xi}}_d(t) + \bar{\boldsymbol{\mathcal{C}}}^T(t)\mathbf{u}_d(t) \tag{25}$$

Again introducing a constant matrix $\bar{\boldsymbol{\mathcal{C}}}_0$, so that the dual system is time-invariant and controllable, a constant gain controller $\bar{\boldsymbol{\mathcal{G}}}_{e,0}$ is designed for the dual system. The periodic observer gain matrix is then given by:

$$\bar{\boldsymbol{\mathcal{G}}}_{obs}^T(t) = [\bar{\boldsymbol{\mathcal{C}}}(t)\bar{\boldsymbol{\mathcal{C}}}^T(t)]^{-1}\bar{\boldsymbol{\mathcal{C}}}(t)\boldsymbol{\mathcal{C}}_0^T\bar{\boldsymbol{\mathcal{G}}}_{e,0} \tag{26}$$

5. Simulation Results

The performance of the designed control methodology is examined by numerical simulations of the coupled rotor-blade system. The parameters of the rotor-blade system used for this numerical analysis are given in Tab. (1).

Table 1: Rotor and blade properties.

Rotor/Hub		**Blades and Tip masses**	
Mass	$m_{hx} = 2.0\,\mathrm{kg}$; $m_{hy} = 2.0\,\mathrm{kg}$	Length	$L_i = 80{\cdot}10^{-3}\,\mathrm{m}$
Stiffness	$K_{x_h} = 6{\cdot}10^3\,\mathrm{N/m}$; $K_{y_h} = 8{\cdot}10^3\,\mathrm{N/m}$	Width	$b_i = 25{\cdot}10^{-3}\,\mathrm{m}$
Damping	$D_{x_h} = 10^{-6}\,\mathrm{N{\cdot}s/m}$; $D_{y_h} = 10^{-6}\,\mathrm{N{\cdot}s/m}$	Thickness	$h_i = 10^{-3}\,\mathrm{m}$
Inertia	$J_h = 10^{-2}\,\mathrm{kg{\cdot}m^2}$	Density	$\rho_i = 0.195\,\mathrm{kg/m}$
Excentricity	$\epsilon = 10^{-3}\,\mathrm{m}$; $\kappa = 0\,\mathrm{rad}$	Elasticity	$E_i = 2.0{\cdot}10^{11}\,\mathrm{N/m^2}$
Diameter	$r = 0.04\,\mathrm{m}$	Locations	$\alpha_i = \frac{(i-1)\pi}{2}\,\mathrm{rad};\ i = 1,2,3,4$
Mass rotor	$m_r = 0.5\,\mathrm{kg}$	Tip mass	$m_{t_i} = 0.105\,\mathrm{kg}$
		Tip inertia	$J_{t_i} = 3.35{\cdot}10^{-5}\,\mathrm{kg{\cdot}m^2}$
		Tip mass length	$L_{t_i} = 2\,r_{t_i} = 30{\cdot}10^{-3}\,\mathrm{m}$
		Damping	$D_{b_i} = 10^{-6}\,\mathrm{N{\cdot}s/m}$
		Inertia	$I_i = \frac{1}{12}b_i h_i^3 = 2.08{\cdot}10^{-12}\,\mathrm{m^4}$

In order to determine a suitable actuator and sensor placement for the considered system, the controllability and observability are analysed for four different actuator and sensor configurations shown in Fig. (2). The actuators can be mounted acting onto the rotor shaft (config. a), acting directly onto the blades (config. b and c) or acting onto both rotor and blades (config. d). Sensors are assumed to be mounted at the same positions to measure the position of the hub or the deflection of the blades at the middle or at the tip point.

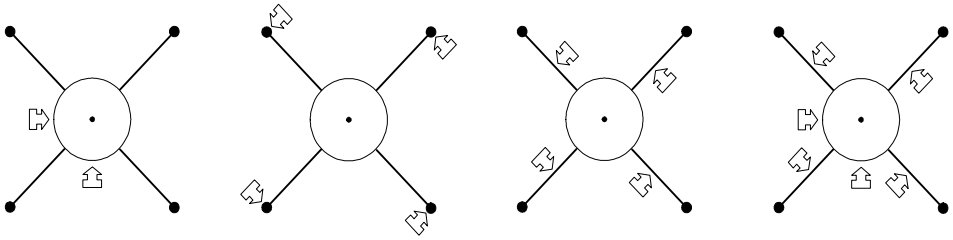

(a) (b) (c) (d)

Figure 2: The four actuator and sensor configurations analysed to obtain optimal actuator and sensor placement.

Table (2) shows the measure of controllability, Eq. (19), for the first 10 modes using the four specified actuator configurations. The indices are normalized referring to the most controllable mode, which is mode 6 for configuration (b), and the higher the controllability index is the more controllable is the mode. The results show that application of only hub based actuation configuration (a) implies that only the modes 1, 2, 5 and 6 can be controlled. For configuration (b) where actuators act at the tip point of the blades, close to the node of the blades 2nd mode shape, the index shows that only the modes related to the blades first mode 3, 4, 5 and 6 can be controlled. For configuration (c) all blade modes, 3 to 10, can be controlled. Finally, it is seen that mounting actuators acting onto both the hub and onto the blades, configuration (d), all 10 modes of the system can be controlled. The normalized result of the equivalent observability analysis, Tab. (3), gives a similar result. Sensors have to be mounted measuring both the hub and the blades movement in order to estimate all state variables.

An alternative method to investigate the controllability and observability of the system is a visual study of the mode shapes. Hereby a physical understanding of the quantitative measures MC and MO can be accomplished. The first 10 mode shapes are visualized in Fig. (3) and observing these shapes the validity of the controllability and observability indices in Tab. (2) and (3) is easily seen. The larger the amplitude of the mode shape is at the location of the actuator

or sensor the more controllable or observable is the mode. Therefore, from these shapes it can directly be seen that, for instance, using only the shaft actuators only the previously mentioned modes can be controlled due to their mode shape amplitude of the rotor. Similarly, can the validity be seen for the other configurations. Consequently, in the numerical example both hub and blade based actuators and sensors are applied to the system. The blade actuators are located at the midpoint of the blades and sensors measure the tip point deflections.

Table 2: Measure of controllability of each mode for the four system configurations with identical blades - MC index.

Actuator	Mode No.									
config.	1	2	3	4	5	6	7	8	9	10
(a)	0.13	0.12	0.00	0.00	0.08	0.07	0.00	0.00	0.00	0.00
(b)	0.04	0.02	0.94	0.94	0.91	1.00	0.04	0.04	0.04	0.04
(c)	0.01	0.01	0.24	0.24	0.23	0.25	0.25	0.25	0.25	0.25
(d)	0.13	0.12	0.24	0.24	0.24	0.26	0.25	0.25	0.25	0.25

Table 3: Measure of observability of each mode for the four system configurations with identical blades - MO index.

Sensor	Mode No.									
config.	1	2	3	4	5	6	7	8	9	10
(a)	1.00	0.82	0.00	0.00	0.04	0.03	0.00	0.00	0.00	0.00
(b)	0.28	0.33	0.48	0.48	0.46	0.44	0.00	0.00	0.00	0.00
(c)	0.07	0.09	0.12	0.12	0.12	0.11	0.03	0.03	0.03	0.03
(d)	1.00	0.83	0.12	0.12	0.12	0.11	0.03	0.03	0.03	0.03

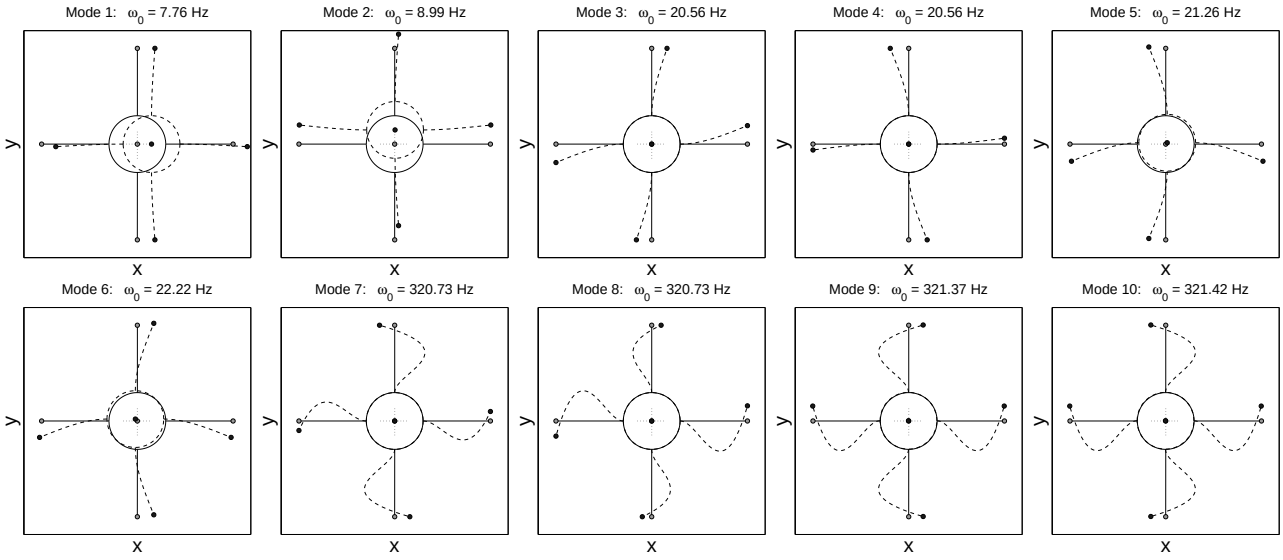

Figure 3: Mode shapes for the coupled rotor-blade system. The frequency ω_0 denotes the basis frequency of the given mode containing also the frequency components $\omega_0 \pm \Omega$ and $\omega_0 \pm 2\Omega$.

Using the order reduction, Eq. (13), an active controller is designed to control the dynamics of specific selected vibration modes, thus treating the remaining modes as residual modes. A model of 10 modes is used for simulation and numerical evaluation of the designed controller performance. Three different controller configurations are designed and examined by numerical simulations. The first controller is designed to control only the first mode, the second controller to reduce all modes primarily related to the first bending mode of the blades (modes 3 to 6) and the third controller to reduce the first six modes of the rotor-blade system. The modes 7 to 10 are considered as residuals in all the controllers. The controller gains are determined by the optimal quadratic control technique minimizing the cost function:

$$J = \int \left(\bar{\boldsymbol{\xi}}^T \mathbf{Q}_\xi \bar{\boldsymbol{\xi}} + \mathbf{u}^T \mathbf{Q}_u \mathbf{u} \right) dt \tag{27}$$

where the elements of the state variable weighting matrix $\mathbf{Q}_\xi$ are given in Tab. (4) and the control input weighting matrix is given by $\mathbf{Q}_u = 10^{-2} \cdot \mathbf{I}_6$. The observer is designed to observe only the modal state variables needed by the controllers. The design weight matrix $\mathbf{Q}_{\xi_d}$ is a diagonal matrix with the values 10^4 for all elements related to the first two modes (1 and 2) and 10^6 for the remaining modes (3 to 6). The input weight matrix is given by $\mathbf{Q}_{u_d} = 10^{-2} \cdot \mathbf{I}_6$.

Table 4: Diagonal elements of the controller design weighting matrix $\mathbf{Q}_\xi$.

	Modes basis frequency $[\mathrm{Hz}]$									
Control	ω_1	ω_2	ω_3	ω_4	ω_5	ω_6	ω_7	ω_8	ω_9	ω_{10}
Scheme	7.76	8.99	20.56	20.56	21.26	22.22	320.73	320.73	321.37	321.42
$\bar{\mathcal{G}}_1$:	10^4	-	-	-	-	-	-	-	-	-
$\bar{\mathcal{G}}_2$:	-	-	10^2	10^2	10^2	10^2	-	-	-	-
$\bar{\mathcal{G}}_3$:	10^4	10^4	10^2	10^2	10^2	10^2	-	-	-	-

Figure (4) shows the transient response of the first six modal state variables for the system without control and when controlled by the three designed control schemes. The rotor-blade system rotates at the constant speed $\Omega = 5\,\mathrm{Hz}$ and the initial conditions of the position state variables are $\mathbf{z}_{ini} = \{-5;\,-5;\,5;\,5;\,-5;\,5\}^T \cdot 10^{-3}\,\mathrm{m}$ and zero velocities $\dot{\mathbf{z}}_{ini} = \mathbf{0}\,\mathrm{m/s}$. The responses might be difficult to differ from each other, however, the plots show the expected responses. The control scheme 1 reduces only the first mode, while the other modal coordinates are almost non-affected. Spill-over effects are observed in the modal state variables 2, 3 and 4. The control scheme 2 reduces only the modes 3, 4, 5 and 6 while the scheme 3 suppresses all six modes efficiently.

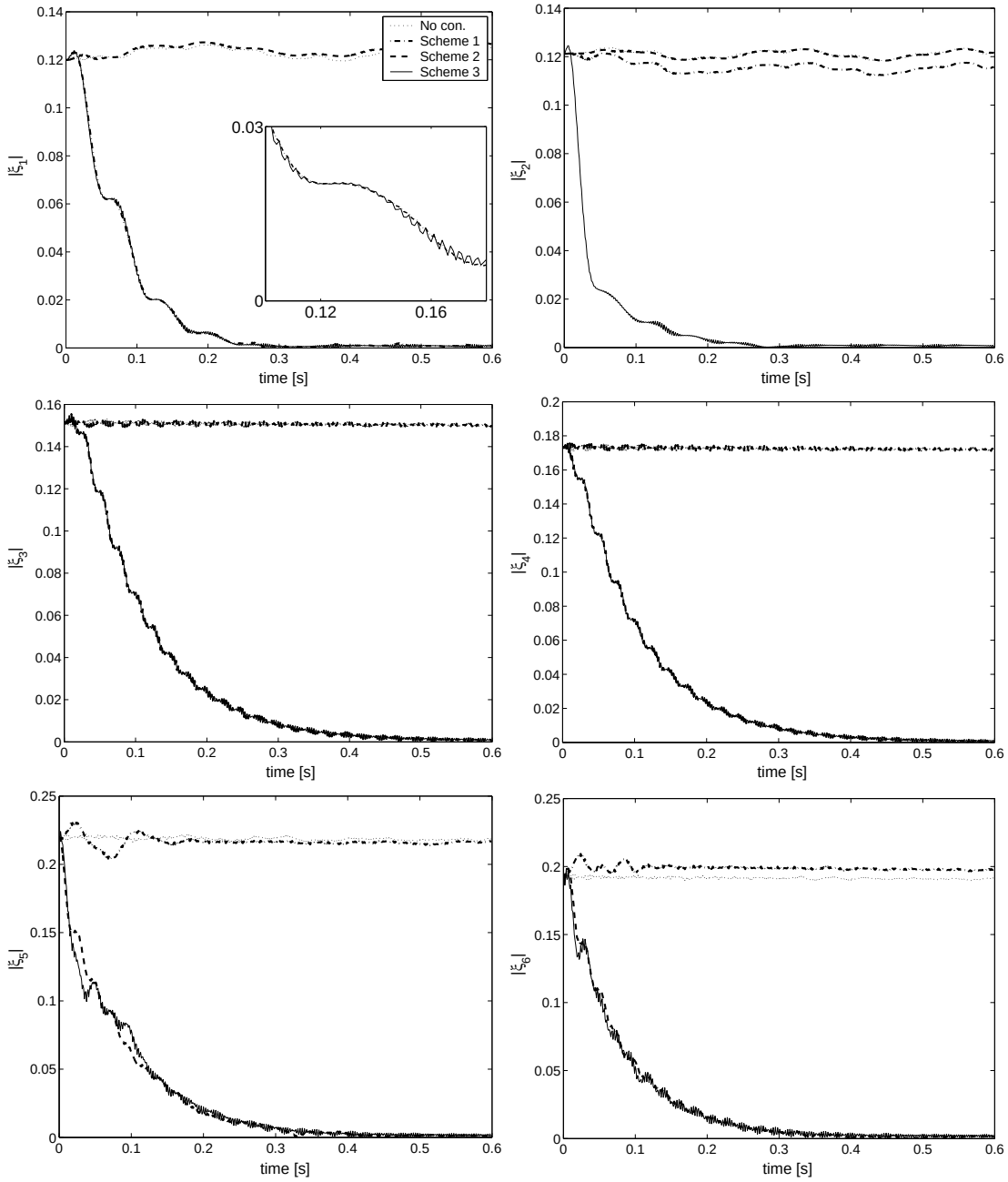

Figure 4: The first six modal state variables of the controlled and non-controlled system.

The Fig. (5) shows the transient response of the rotor position and the blade 2 deflection (x_h, y_h and d_2) and the applied control forces of the system without control and when controlled by the three designed control schemes. The mode 1 mostly contributes to the hub movement in the x-direction, therefore, the control scheme 1 primarily reduces this movement. However, due to the vibration coupling among the rigid rotor and the blades, parametric vibration modes appear in the response (Saracho and Santos, 2003). This implies that the first mode of the system is not purely related to the hub movement in the x-direction, but also slightly to the blades motion, see Fig. (3). Therefore, also the blade deflection is very slightly affected when controlling the first mode. For control scheme 2 only the blades motion primarily related to the modes 3, 4, 5 and 6 are suppressed but the hub movements are slightly affected due to the coupling. For control scheme 3 the transient responses show that the vibrations of x_h, y_h and d_2 are all very efficiently suppressed.

Figure (6) shows the frequency response function for the system subjected to an impulse excitation. Again the lines of the spectra might be difficult to differ from each other because they are coincident in some cases. The spectra show that primarily the modes addressed by the controllers are affected and suppressed. Furthermore, the presence of parametric vibration modes in the dynamic response, due to the vibration coupling, is observed by the peaks arising at the frequencies $\omega_1 \pm \Omega$, $\omega_2 \pm \Omega$, $\omega_5 - \Omega$ and $\omega_6 + \Omega$.

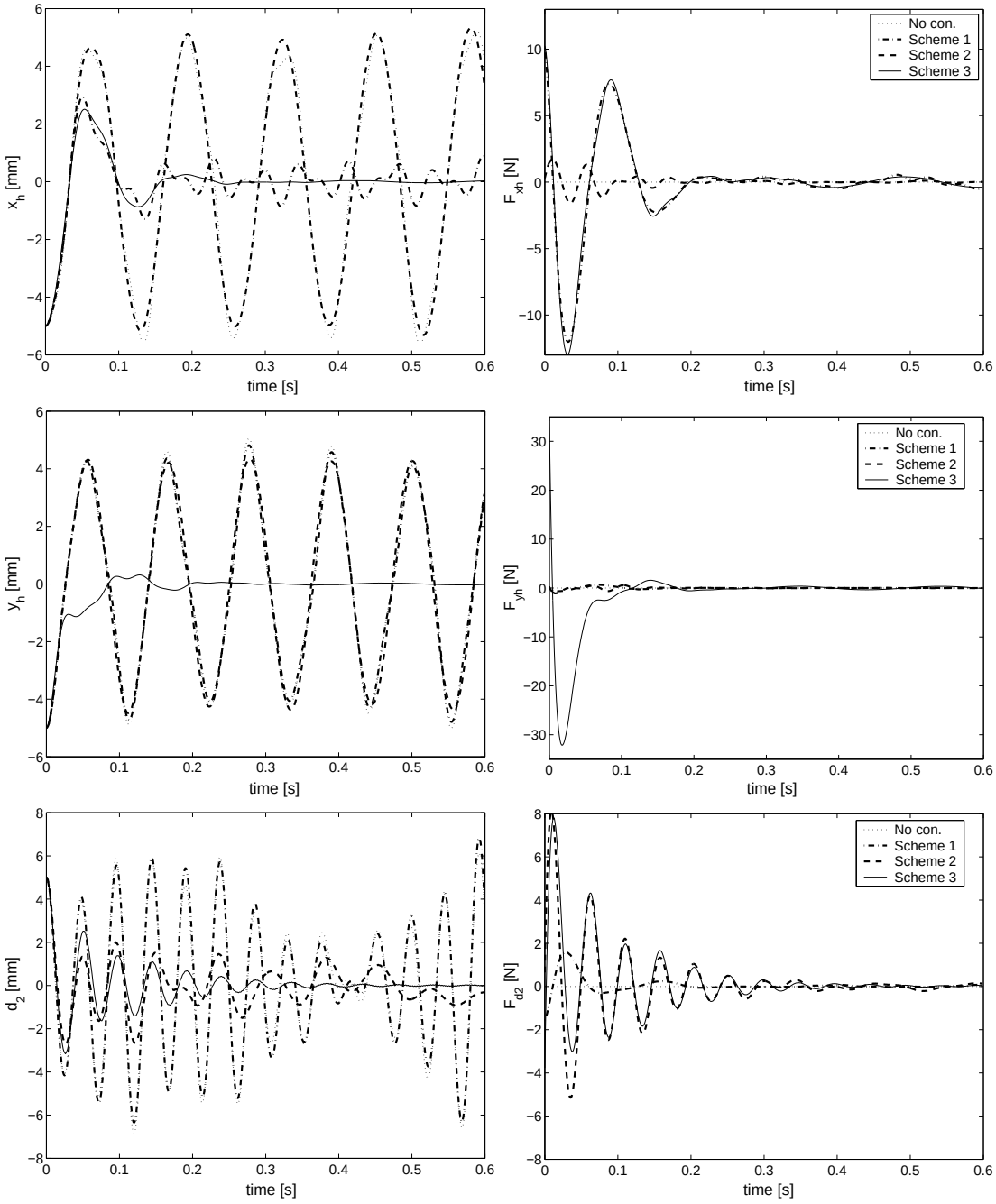

Figure 5: Hub movement, tip point deflection of blade 2 and the control force applied to the system using the three designed control schemes.

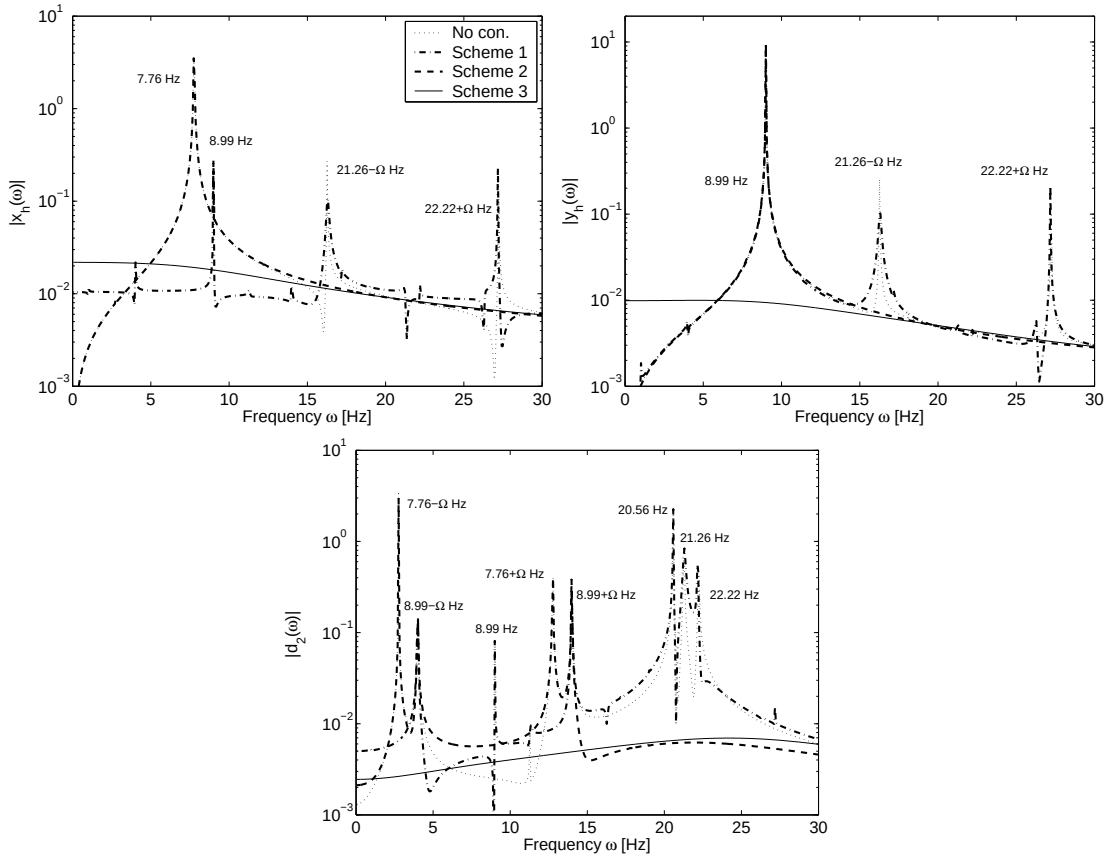

Figure 6: Frequency spectrum diagrams for the rotor-blade system controlled by the three control schemes and without control.

6. Conclusion

A methodology for designing a periodic time-variant modal controller for vibration suppression in a coupled rotor-blade system is presented. The results obtained reveals that using a periodic modal transformation a periodic controller can be designed with help of the traditional linear time-invariant control technique. The applicability and effectiveness of the designed control methodology is numerically examined by controlling the vibrations of a periodic time-variant coupled rotor-blade system. Such numerical investigations demonstrate that the vibrations can be efficiently reduced and that specific selected vibration modes can be separately attenuated.

The modal transformation of the periodic system provides a very effective tool for analysing the system modal controllability and observability, which are very useful to identify suitable locations for sensors and actuators. For the considered rotor-blade system with four identical blades it is necessary to implement actuators acting onto both the hub and onto each blade in order to control and observe all state variables.

7. References

Arcara, P. & Bittanti, S. & Lovera, M: *Periodic Control of Helicopter Rotors for Attenuation of Vibrations in Forward Flight*, IEEE transactions on control systems technology, Vol. 8, No. 6, 2000.

Balas, M.J.: *Modal Control of Certain Flexible Dynamic Systems*, SIAM Journal of Control and Optimization, Vol. 16, No. 3, pp. 450-462, 1978.

Bittanti, S. & Cuzzola, F.A.: *Periodic Active Control of Vibrations in Helicopters: A Gain-Scheduled Multi-Objective Approach*, Control Engineering Practice, Vol. 10, pp. 1043-1057, 2002.

Calico, R.A. & Wiesel, W.E.: *Control of Time-Periodic Systems*, Journal of Guidance, Control and Dynamics, Vol. 7, No. 6, pp. 671-676, 1984.

Calise, A.J. & Wasikowski, M.E. & Schrage, D.P: *Optimal Output Feedback for Linear Time-Periodic Systems*, Journal of Guidance, Control and Dynamics, Vol. 15, No. 2, pp. 416-423, 1992.

Chantalakhana, C. & Stanway, R.: *Active Constrained Layer Damping of Plate Vibrations: A Numerical and Experimental Study of Modal Controllers*, Smart Materials and Structures, Vol. 9, pp. 940-952, 2000.

Firoozian, R. & Stanway, R.: *Active Vibration Control of Turbomachinery: A Numerical Investigation of Modal Controllers*, Mechanical Systems and Signal Processing, 2(3), pp. 243-264, 1988.

Hamdan, A.M.A. & Nayfeh, A.H.: *Measure of Modal Controllability and Observability for First- and Second-Order Linear Systems*, Journal of Guidance, Control and Dynamics, Vol. 12, No. 3, pp. 421-428, 1989.

Kaneko, J. & Kano, H.: *Modal Control of Flexible One-Link Arms with Random Disturbances*, IEEE Proceedings of the 28th Conference on Decision and Control, pp. 2141-2146, 1989.

Khulief, Y.A.: *Vibration Suppression in Rotating Beams Using Active Modal Control*, Journal of Sound and Vibration, Vol. 242, No. 4, pp. 681-699, 2001.

Marghitu, D.B. & Sinha, S.C. & Diaconescu, C.: *Control of a Parametrically Excited Flexible Beam Undergoing Rotation and Impacts*, Multibody System Dynamics, (3), pp. 47-63, 1999.

Saracho, C.M. & Santos, I. F.: *Dynamic models for coupled blade-rotor vibrations*, Procedings of the IX DINAME, pp. 263-268, 2001.

Saracho, C.M. & Santos, I.F.: *Modal analysis in periodic, time-varying systems with emphasis to the coupling between flexible rotating beams and non-rotating flexible structures*, Procedings of the X DINAME, pp. 399-404, 2003.

Sinha, S.C. & Joseph, P.: *Control of General Dynamic Systems With Periodically Varying Parameters Via Liapunov-Floquet Transformation*, Journal of Dynamic Systems, Measurement and Control, Vol. 116, pp. 650-658, 1994.

Szász, G. & Flowers, G.T.: *Time Periodic Control of a Bladed Disk Assembly Using Shaft Based Actuation*, Journal of Vibration and Acoustics, Vol. 123, pp. 395-401, July 2001.

Xu, J. & Gasch, R.: *Modale behandlung linearer periodisch zeitvarianter bewegungsgleichungen*, Archive of Applied Mechanics, Vol. 65, No. 3, pp. 178-193, 1995, (in german).

A. Equations of Motion

Blade mode shape functions:

$$\varphi_{1i}(x_i) = -7.60\cdot 10^{2}\, x_i^3 + 2.17\cdot 10^{2}\, x_i^2 + 8.65\cdot 10^{-3}\, x_i \quad ; \quad \varphi_{2i}(x_i) = -6.70\cdot 10^{4}\, x_i^4 + 2.52\cdot 10^{4}\, x_i^3 + -1.77\cdot 10^{3}\, x_i^2 + 1.57\cdot 10^{0}\, x_i$$

Temporary variables:

$$\mathbf{\Psi} = \left\{ \begin{array}{c} m_{t_i}\left(\varphi_{1i}(L_i) + r_{t_i}\varphi'_{1i}(L_i)\right) + \rho_i \int_0^{L_i} \varphi_{1i}(x_i)dx_i \\ m_{t_i}\left(\varphi_{2i}(L_i) + r_{t_i}\varphi'_{2i}(L_i)\right) + \rho_i \int_0^{L_i} \varphi_{2i}(x_i)dx_i \end{array} \right\}^T \quad ; \quad \sin_i = \sin(\theta+\alpha_i) \quad ; \quad \cos_i = \cos(\theta+\alpha_i)$$

Matrices of the dynamic model Eq. 8:

$$\mathbf{M} = \begin{bmatrix} m_{h_x} + \sum_{i=1}^{4}\left(m_{t_i} + \rho_i L_i\right) & 0 & -\mathbf{\Psi}\sin_1 & -\mathbf{\Psi}\sin_2 & -\mathbf{\Psi}\sin_3 & -\mathbf{\Psi}\sin_4 \\ 0 & m_{h_y} + \sum_{i=1}^{4}\left(m_{t_i} + \rho_i L_i\right) & \mathbf{\Psi}\cos_1 & \mathbf{\Psi}\cos_2 & \mathbf{\Psi}\cos_3 & \mathbf{\Psi}\cos_4 \\ -\mathbf{\Psi}^T\sin_1 & \mathbf{\Psi}^T\cos_1 & \mathbf{M}_{q_1q_1} & \mathbf{0} & \mathbf{0} & \mathbf{0} \\ -\mathbf{\Psi}^T\sin_2 & \mathbf{\Psi}^T\cos_2 & \mathbf{0} & \mathbf{M}_{q_2q_2} & \mathbf{0} & \mathbf{0} \\ -\mathbf{\Psi}^T\sin_3 & \mathbf{\Psi}^T\cos_3 & \mathbf{0} & \mathbf{0} & \mathbf{M}_{q_3q_3} & \mathbf{0} \\ -\mathbf{\Psi}^T\sin_4 & \mathbf{\Psi}^T\cos_4 & \mathbf{0} & \mathbf{0} & \mathbf{0} & \mathbf{M}_{q_4q_4} \end{bmatrix} \quad ; \quad \mathbf{M}_{q_iq_i} = \begin{bmatrix} m_{11} & m_{12} \\ m_{21} & m_{22} \end{bmatrix}$$

$$m_{vw} = m_{t_i}\varphi_{vi}(L_i)\varphi_{wi}(L_i) + \left(J_{t_i} + m_{t_i}r_{t_i}^2\right)\varphi'_{vi}(L_i)\varphi'_{wi}(L_i) + m_{t_i}r_{t_i}\left(\varphi'_{vi}(L_i)\varphi_{wi}(L_i) + \varphi_{vi}(L_i)\varphi'_{wi}(L_i)\right) + \int_0^{L_i}\rho_i\varphi_{vi}(x_i)\varphi_{wi}(x_i)dx_i$$

$$\mathbf{H} = \begin{bmatrix} \mathrm{D}_{x_h} & 0 & -2\dot\theta\mathbf{\Psi}\cos_1 & -2\dot\theta\mathbf{\Psi}\cos_2 & -2\dot\theta\mathbf{\Psi}\cos_3 & -2\dot\theta\mathbf{\Psi}\cos_4 \\ 0 & \mathrm{D}_{y_h} & -2\dot\theta\mathbf{\Psi}\sin_1 & -2\dot\theta\mathbf{\Psi}\sin_2 & -2\dot\theta\mathbf{\Psi}\sin_3 & -2\dot\theta\mathbf{\Psi}\sin_4 \\ \mathbf{0} & \mathbf{0} & \mathbf{D}_{q_1q_1} & \mathbf{0} & \mathbf{0} & \mathbf{0} \\ \mathbf{0} & \mathbf{0} & \mathbf{0} & \mathbf{D}_{q_2q_2} & \mathbf{0} & \mathbf{0} \\ \mathbf{0} & \mathbf{0} & \mathbf{0} & \mathbf{0} & \mathbf{D}_{q_3q_3} & \mathbf{0} \\ \mathbf{0} & \mathbf{0} & \mathbf{0} & \mathbf{0} & \mathbf{0} & \mathbf{D}_{q_4q_4} \end{bmatrix} \quad ; \quad \mathbf{D}_{q_iq_i} = \begin{bmatrix} D_{b_i} & 0 \\ 0 & D_{b_i} \end{bmatrix}$$

$$\mathbf{K} = \begin{bmatrix} \mathrm{K}_{x_h} & 0 & \mathbf{\Psi}(\dot\theta^2\sin_1 - \ddot\theta\cos_1) & \mathbf{\Psi}(\dot\theta^2\sin_2 - \ddot\theta\cos_2) & \mathbf{\Psi}(\dot\theta^2\sin_3 - \ddot\theta\cos_3) & \mathbf{\Psi}(\dot\theta^2\sin_4 - \ddot\theta\cos_4) \\ 0 & \mathrm{K}_{y_h} & \mathbf{\Psi}(-\dot\theta^2\cos_1 - \ddot\theta\sin_1) & \mathbf{\Psi}(-\dot\theta^2\cos_2 - \ddot\theta\sin_2) & \mathbf{\Psi}(-\dot\theta^2\cos_3 - \ddot\theta\sin_3) & \mathbf{\Psi}(-\dot\theta^2\cos_4 - \ddot\theta\sin_4) \\ \mathbf{0} & \mathbf{0} & \mathbf{K}_{q_1q_1} & \mathbf{0} & \mathbf{0} & \mathbf{0} \\ \mathbf{0} & \mathbf{0} & \mathbf{0} & \mathbf{K}_{q_2q_2} & \mathbf{0} & \mathbf{0} \\ \mathbf{0} & \mathbf{0} & \mathbf{0} & \mathbf{0} & \mathbf{K}_{q_3q_3} & \mathbf{0} \\ \mathbf{0} & \mathbf{0} & \mathbf{0} & \mathbf{0} & \mathbf{0} & \mathbf{K}_{q_4q_4} \end{bmatrix} \quad ; \quad \mathbf{K}_{q_iq_i} = \begin{bmatrix} k_{11} & k_{12} \\ k_{21} & k_{22} \end{bmatrix}$$

$$\begin{aligned} k_{vw} = & \int_0^{L_i} E_i I_i \varphi''_{vi}(x_i)\varphi''_{wi}(x_i)dx_i - \dot\theta^2\left(m_{t_i}\varphi_{vi}(L_i)\varphi_{wi}(L_i) + m_{t_i}r_{t_i}^2\varphi'_{vi}(L_i)\varphi'_{wi}(L_i) + m_{t_i}r_{t_i}\left(\varphi_{vi}(L_i)\varphi'_{wi}(L_i)\right.\right. \\ & \left.\left. + \varphi'_{vi}(L_i)\varphi_{wi}(L_i)\right) + \int_0^{L_i}\rho_i\varphi_{vi}(x_i)\varphi_{wi}(x_i)dx_i - (L_i + r + r_{t_i})m_{t_i}\int_0^{L_i}\varphi'_{vi}(x_i)\varphi'_{wi}(x_i)dx_i \right. \\ & \left. - \rho_i\int_0^{L_i}(L_i - x_i)(r + x_i)\varphi'_{vi}(x_i)\varphi'_{wi}(x_i)dx_i\right) - g\left(\sin_i\int_0^{L_i}\left(m_{t_i} + \rho_i(L_i - x_i)\right)\varphi'_{vi}(L_i)\varphi'_{wi}(L_i)dx_i\right) \end{aligned}$$

$$\mathbf{P} = \left\{ \begin{array}{ccccccc} \mathrm{P}_{x_h}; & \mathrm{P}_{y_h}; & \mathbf{P}_{q1}; & \mathbf{P}_{q2}; & \mathbf{P}_{q3}; & \mathbf{P}_{q4} \end{array} \right\}^T$$

$$\mathrm{P}_{x_h} = \epsilon m_{rx}(\dot\theta^2\cos(\theta+\kappa) + \ddot\theta\sin(\theta+\kappa)) + \sum_{i=1}^{4}(\dot\theta^2\cos_i + \ddot\theta\sin_i)\left(m_{t_i}(r + L_i + r_{t_i}) + \rho_i L_i(\tfrac{1}{2}L_i + r)\right)$$

$$\mathrm{P}_{y_h} = \epsilon m_{rx}(\dot\theta^2\sin(\theta+\kappa) - \ddot\theta\cos(\theta+\kappa)) + \sum_{i=1}^{4}(\dot\theta^2\sin_i - \ddot\theta\cos_i)\left(m_{t_i}(r + L_i + r_{t_i}) + \rho_i L_i(\tfrac{1}{2}L_i + r)\right) - g\left(m_{h_y} + \sum_{i=1}^{4}m_{t_i} + \rho_i L_i\right)$$

$$\mathbf{P}_{q_i} = -g\mathbf{\Psi}\cos_i - \ddot\theta\left\{ \begin{array}{c} m_{t_i}(r + L_i + r_{t_i})\left(\varphi_{1i}(L_i) + r_{t_i}\varphi'_{1i}(L_i)\right) + J_{t_i}\varphi'_{1i}(L_i) + \rho\int_0^{L_i}(r + x_i)\varphi_{1i}(x_i)dx_i \\ m_{t_i}(r + L_i + r_{t_i})\left(\varphi_{2i}(L_i) + r_{t_i}\varphi'_{2i}(L_i)\right) + J_{t_i}\varphi'_{2i}(L_i) + \rho\int_0^{L_i}(r + x_i)\varphi_{2i}(x_i)dx_i \end{array} \right\}^T$$

$$\mathbf{Q} = \begin{bmatrix} 1 & 0 & 0 & 0 & 0 & 0 \\ 0 & 1 & 0 & 0 & 0 & 0 \\ \mathbf{0} & \mathbf{0} & \mathbf{Q}_{q1} & \mathbf{0} & \mathbf{0} & \mathbf{0} \\ \mathbf{0} & \mathbf{0} & \mathbf{0} & \mathbf{Q}_{q2} & \mathbf{0} & \mathbf{0} \\ \mathbf{0} & \mathbf{0} & \mathbf{0} & \mathbf{0} & \mathbf{Q}_{q3} & \mathbf{0} \\ \mathbf{0} & \mathbf{0} & \mathbf{0} & \mathbf{0} & \mathbf{0} & \mathbf{Q}_{q4} \end{bmatrix} \quad ; \quad \mathbf{Q}_{q_i} = \left\{ \begin{array}{c} \varphi_{1i}(l_m) \\ \varphi_{2i}(l_m) \end{array} \right\}$$

State space output matrix:

$$\mathbf{C}_{(N_m\times 2N_c)} = \begin{bmatrix} 1 & 0 & 0 & 0 & 0 & 0 \\ 0 & 1 & 0 & 0 & 0 & 0 \\ \mathbf{0} & \mathbf{0} & \boldsymbol{\varphi}_1(L_1) & \mathbf{0} & \mathbf{0} & \mathbf{0} \\ \mathbf{0} & \mathbf{0} & \mathbf{0} & \boldsymbol{\varphi}_2(L_2) & \mathbf{0} & \mathbf{0} \\ \mathbf{0} & \mathbf{0} & \mathbf{0} & \mathbf{0} & \boldsymbol{\varphi}_3(L_3) & \mathbf{0} \\ \mathbf{0} & \mathbf{0} & \mathbf{0} & \mathbf{0} & \mathbf{0} & \boldsymbol{\varphi}_4(L_4) \\ & & & \mathbf{0}_{N\times 6} & & \end{bmatrix}^T$$